**Cell Reports, Volume *41***

## Supplemental information

# Inhibition of HCK in myeloid cells restricts pancreatic tumor growth and metastasis

**Ashleigh R. Poh, Megan O'Brien, David Chisanga, Hong He, David Baloyan, Jasmin Traichel, Christine Dijkstra, Michaël Chopin, Stephen Nutt, Lachlan Whitehead, Louis Boon, Ashleigh Parkin, Clifford Lowell, Marina Pajic, Wei Shi, Mehrdad Nikfarjam, and Matthias Ernst**

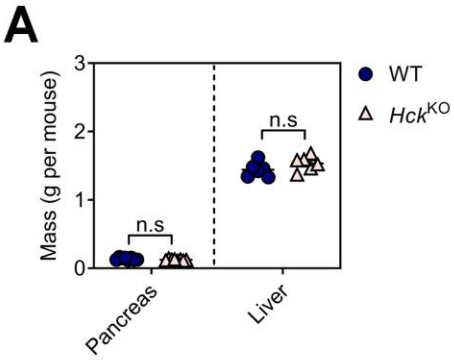
A
Mass (g per mouse)
3
2
1
0
n.s
n.s
WT
Hck^KO
Pancreas
Liver

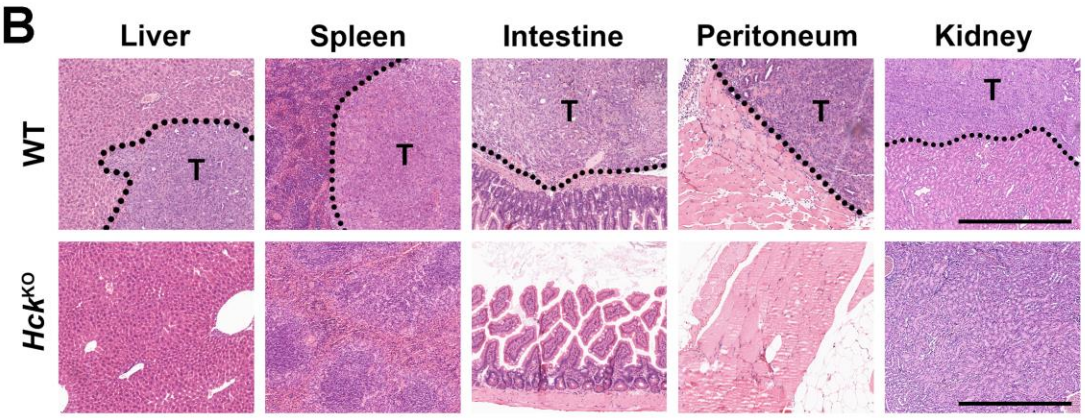
B
Liver
Spleen
Intestine
Peritoneum
Kidney
WT
Hck^KO
T

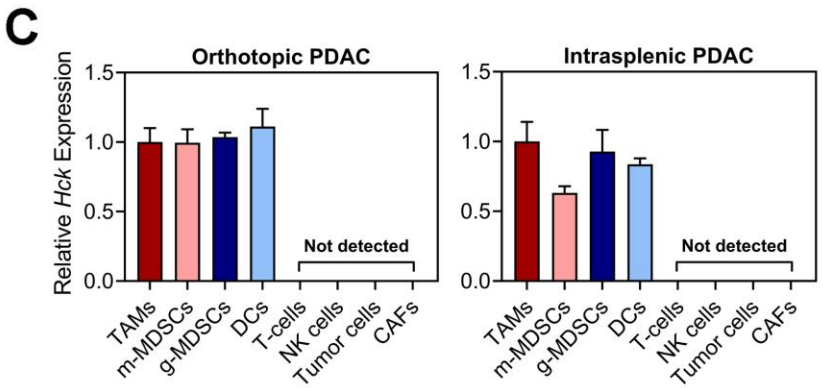
C
Orthotopic PDAC
Intrasplenic PDAC
Relative Hck Expression
1.5
1.0
0.5
0.0
Not detected
TAMs
m-MDSCs
g-MDSCs
DCs
T-cells
NK cells
Tumor cells
CAFs

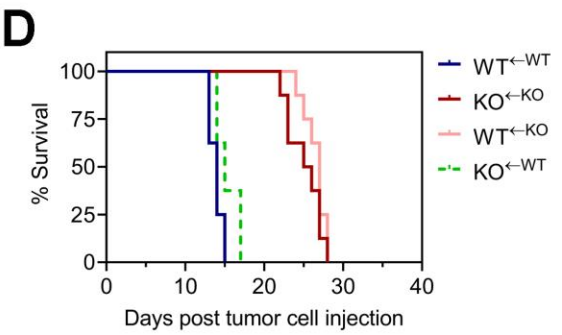
D
% Survival
100
75
50
25
0
0
10
20
30
40
Days post tumor cell injection
WT←WT
KO←KO
WT←KO
KO←WT

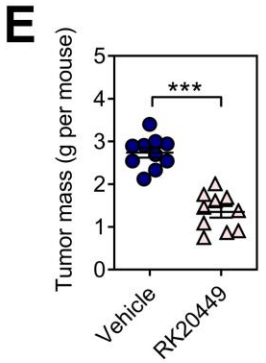
E
Tumor mass (g per mouse)
5
4
3
2
1
0
***
Vehicle
RK20449

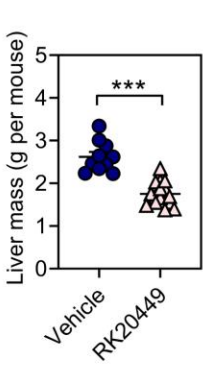
F
Liver mass (g per mouse)
5
4
3
2
1
0
***
Vehicle
RK20449

**Figure S1. *HCK* expression is restricted to the myeloid cell compartment of mouse and human PDAC. Related to Figure 1.**

**(A)** Pancreas and liver weights of treatment naïve WT and *Hck*$^{KO}$ hosts. Each symbol represents an individual mouse. n ≥ 6 mice per group.

**(B)** Representative H&E sections of secondary organs from WT and *Hck*$^{KO}$ hosts (n ≥ 11 mice per group) as described in Figure 1D. T: tumor. Dotted lines indicate tumor boundary. Scale bar: 100μm.

**(C)** *Hck* gene expression in TAMs ($CD45^+CD11b^+F4/80^+$), m-MDSCs ($CD45^+CD11b^+Ly6c^+Ly6g^-$), g-MDSCs ($CD45^+CD11b^+Ly6c^{int}Ly6g^+$), DCs ($CD45^+CD11c^+F4/80^-MHCII^+$), T-cells ($CD45^+TCR\beta^+$), NK cells ($CD45^+NK1.1^+$), cancer cells ($EpCAM^+CD45^-$), and CAFs ($CD45^-EpCAM^-CD31^-PDPN^+PDGFR\alpha^+$) isolated from orthotopic and intrasplenic KPC tumors. n = 4 mice per group.

**(D)** Kaplan-Meier survival analysis of WT and *Hck*$^{KO}$ bone marrow chimeras (Recipient$^{\leftarrow Donor}$) following intrasplenic injection of KPC tumor cells. n = 8 mice per group. A Mantel-Cox log-rank test was used to evaluate statistical significance (see Table S1).

**(E)** Mass of primary PDAC tumors from WT hosts treated twice daily with vehicle or the small molecule HCK inhibitor RK20449. Treatment commenced 1 week after orthotopic injection of KPC tumor cells and continued for 4 weeks. Each symbol represents an individual mouse. n = 10 mice per group.

**(F)** Quantification of metastatic tumor burden by liver weight in WT hosts treated twice daily with vehicle or the small molecule HCK inhibitor RK20449. Treatment commenced on the 5$^{th}$ day after intrasplenic KPC tumor cell injection and continued for 2 weeks. Each symbol represents an individual mouse. n ≥ 10 mice per group.

Data represents mean ± SEM; ***p < 0.001, n.s not significant, with statistical significance determined by an unpaired Student's T-test for comparison between two means.

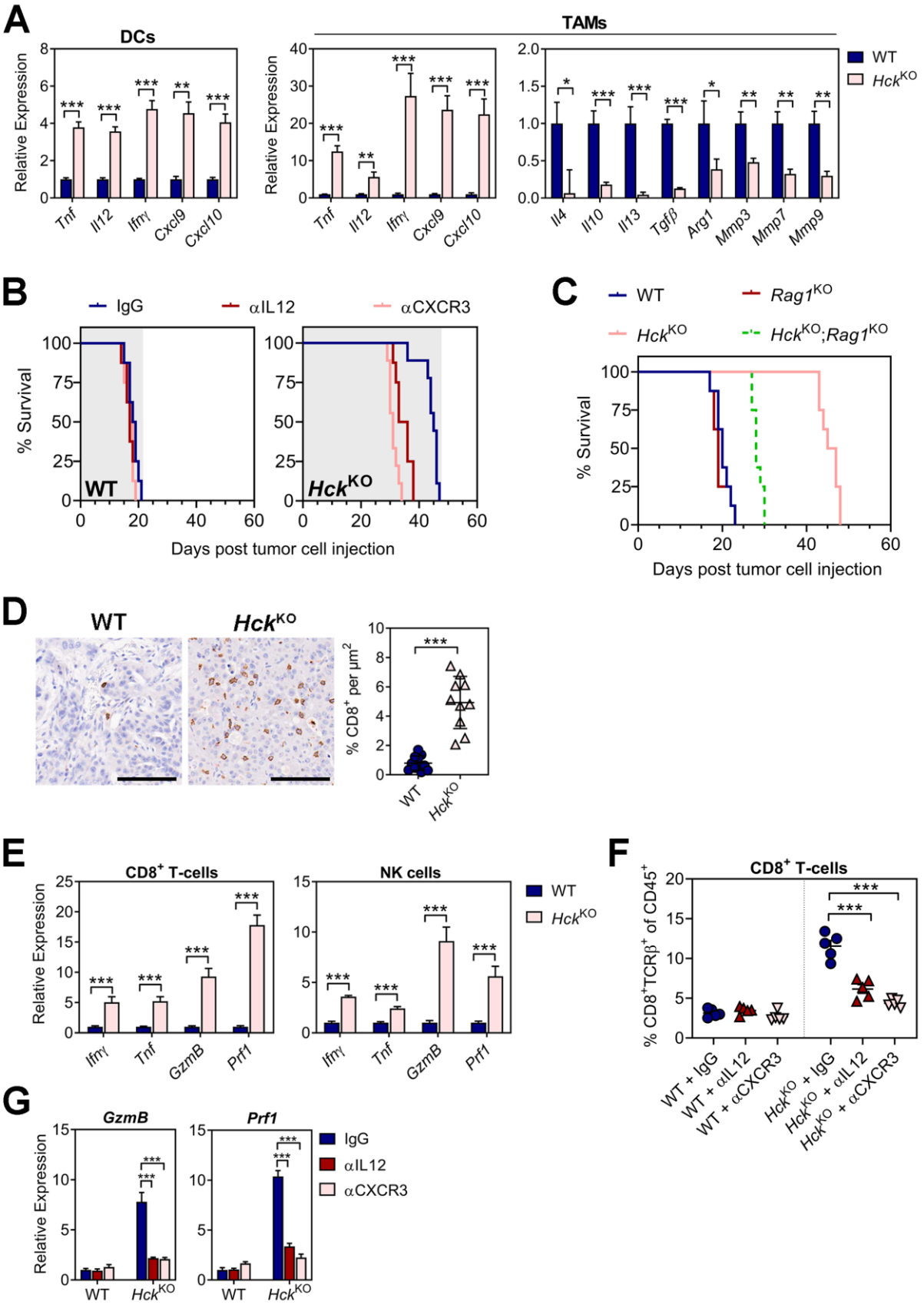
A
DCs
TAMs
Relative Expression
WT
Hck^KO
Tnf
Il12
Ifnγ
Cxcl9
Cxcl10
Il4
Il10
Il13
Tgfβ
Arg1
Mmp3
Mmp7
Mmp9
B
IgG
αIL12
αCXCR3
% Survival
WT
Hck^KO
Days post tumor cell injection
C
WT
Rag1^KO
Hck^KO
Hck^KO;Rag1^KO
% Survival
Days post tumor cell injection
D
WT
Hck^KO
% CD8+ per μm2
E
CD8+ T-cells
NK cells
Relative Expression
Ifnγ
Tnf
GzmB
Prf1
F
CD8+ T-cells
% CD8+TCRβ+ of CD45+
WT + IgG
WT + αIL12
WT + αCXCR3
Hck^KO + IgG
Hck^KO + αIL12
Hck^KO + αCXCR3
G
GzmB
Prf1
Relative Expression
IgG
αIL12
αCXCR3

**Figure S2. Genetic ablation of HCK in myeloid cells promotes immune cell activation. Related to Figure 2.**

**(A)** qPCR analysis on $CD45^{+}CD11c^{+}F4/80^{-}MHCII^{+}$ DCs and $CD45^{+}CD11b^{+}F4/80^{High}Ly6c^{-}Ly6g^{-}$ TAMs isolated from KPC liver metastases of WT and *Hck*$^{KO}$ hosts for genes associated with immune cell activation (i.e., *Tnf*, *Il12*, *Ifny*, *Cxcl9*, *Cxcl10*), immune-suppression (i.e., *Il4*, *Il10*, *Il13*, *Tgfβ*, *Arg1*) and matrix remodeling (i.e., *Mmp3, Mmp7, Mmp9*). n ≥ 6 mice per group.

**(B)** Kaplan-Meier survival analysis of tumor-bearing WT and *Hck*$^{KO}$ hosts treated with αIL12, αCXCR3, or a matched IgG isotype control until clinical endpoint. Shaded area indicates treatment period. n ≥ 8 mice per group. A Mantel-Cox log-rank test was used to evaluate statistical significance (see Table S2).

**(C)** Kaplan-Meier survival analysis of WT, *Hck*$^{KO}$ and lymphocyte-deficient *Rag1*$^{KO}$ and *Hck*$^{KO}$;*Rag1*$^{KO}$ hosts following intrasplenic injection of KPC tumor cells. n = 8 mice per group. A Mantel-Cox log-rank test was used to evaluate statistical significance (see Table S4).

**(D)** Representative immunohistochemical staining and quantification of $CD8^{+}$ T-cells in KPC liver metastases of WT and *Hck*$^{KO}$ hosts. Scale bar: 100μm. Each symbol represents an individual mouse. n ≥ 10 mice per group.

**(E)** qPCR analysis on $CD45^{+}TCR\beta^{+}CD8^{+}$ T-cells and $CD45^{+}NK1.1^{+}$ NK cells isolated from KPC liver metastases of WT and *Hck*$^{KO}$ hosts for genes associated with immune cell activation. n = 7 mice per group.

**(F)** Flow cytometry quantification of $CD8^{+}$ T-cells from KPC liver metastases of WT and *Hck*$^{KO}$ hosts treated with αIL12, αCXCR3, or a matched IgG isotype control for 3 weeks. Each symbol represents an individual mouse. n = 5 mice per group.

**(G)** qPCR analysis on $CD45^{+}TCR\beta^{+}CD8^{+}$ T-cells isolated from KPC liver metastases of WT and *Hck*$^{KO}$ hosts treated with αIL12, αCXCR3, or a matched IgG isotype control for 3 weeks. n = 4 mice per group.

Data represents mean ± SEM; *p < 0.05, **p < 0.01, ***p < 0.001, with statistical significance determined by an unpaired Student's T-test for comparison between two means or one-way ANOVA followed by Tukey's multiple comparison test for comparison between multiple groups.

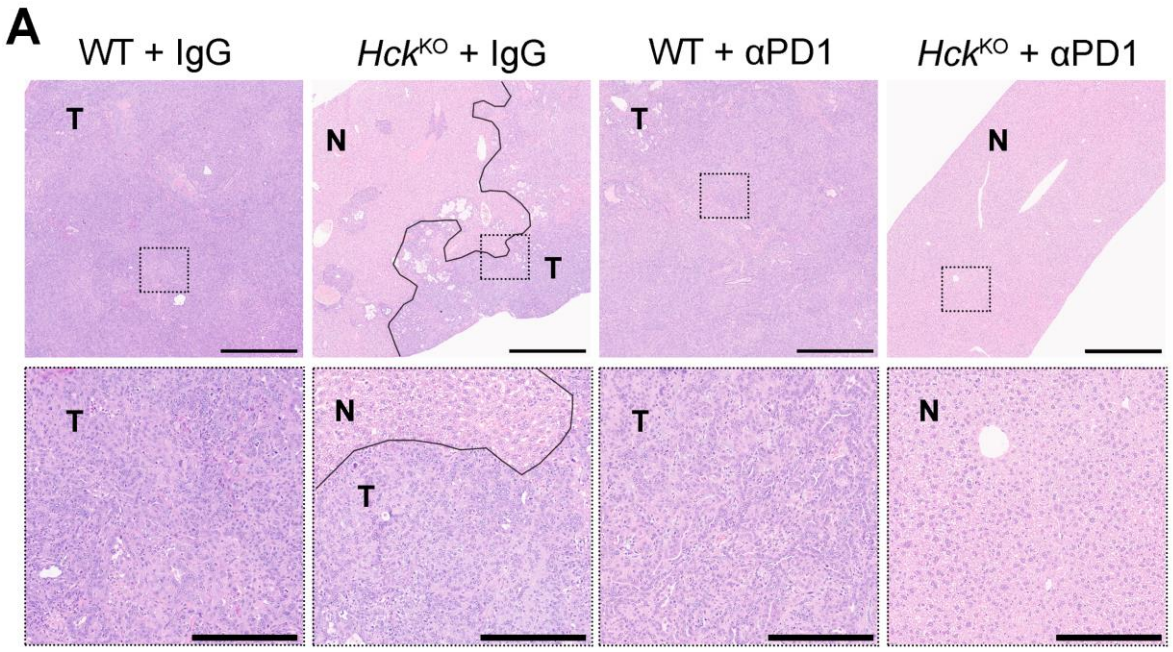
A
WT + IgG
Hck^KO + IgG
WT + αPD1
Hck^KO + αPD1
T
N
T
N
T
N
T
N
T
N
T
N

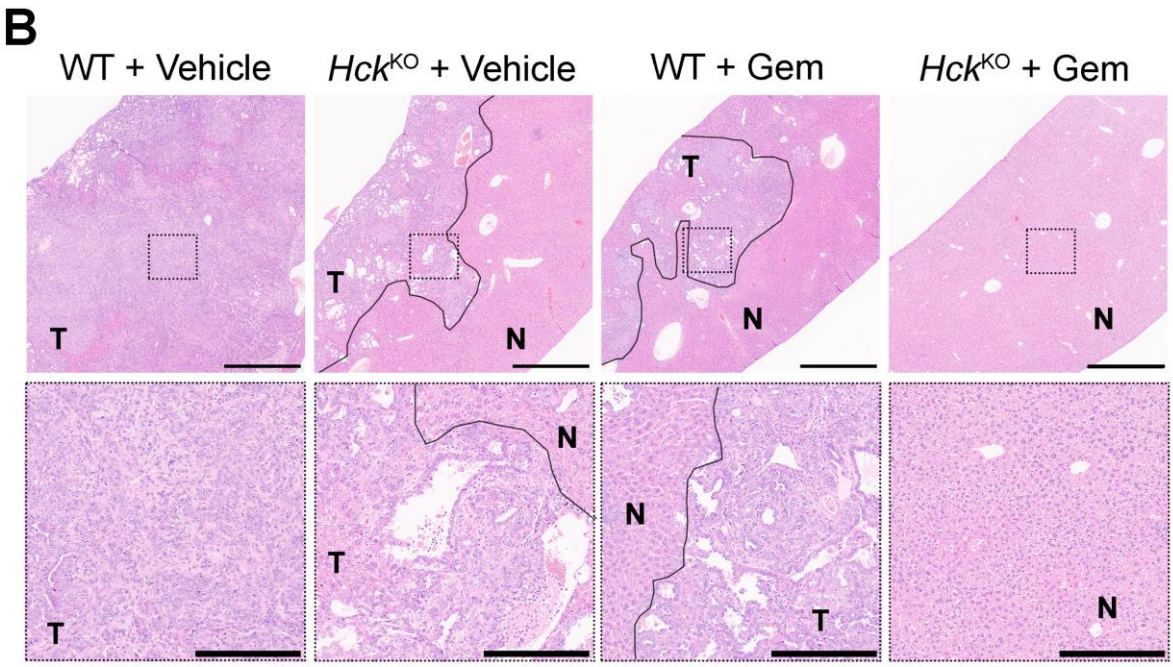
B
WT + Vehicle
Hck^KO + Vehicle
WT + Gem
Hck^KO + Gem
T
T
N
T
N
N
N
T
N
T
N
N
T
N

**Figure S3. Genetic ablation of HCK in myeloid cells overcomes resistance to immunotherapy and improves the efficacy of chemotherapy in PDAC. Related to Figure 4.**

**(A)** Representative H&E-stained liver sections from WT and *Hck*$^{KO}$ hosts (n ≥ 15 mice per group) treated once every 3 days with αPD1 or a matched IgG isotype control. Treatment commenced on the 5$^{th}$ day after intrasplenic KPC tumor cell injection and continued for 2 weeks. A solid black line separates tumor (T) and normal tissue (N). Scale bar of top panel: 2mm, Scale bar of bottom panel (dotted insets): 300μm.

**(B)** Representative H&E-stained liver sections from WT and *Hck*$^{KO}$ hosts (n ≥ 10 mice per group) treated twice weekly with Gemcitabine or PBS vehicle. Treatment commenced on the 5$^{th}$ day after intrasplenic KPC tumor cell injection and continued for 2 weeks. A solid black line separates tumor (T) and normal tissue (N). Scale bar of top panel: 2mm, Scale bar of bottom panel (dotted insets): 300μm.

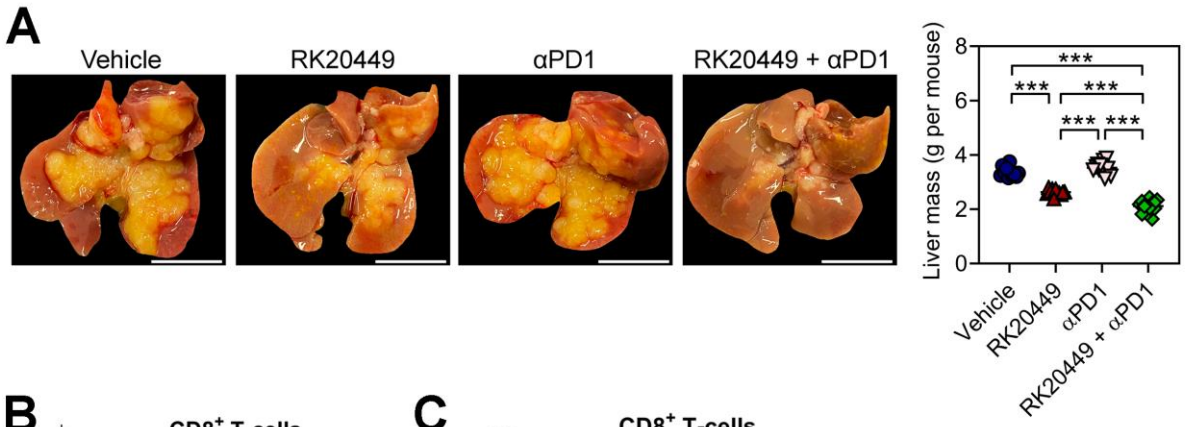
A
Vehicle
RK20449
αPD1
RK20449 + αPD1
Liver mass (g per mouse)
Vehicle
RK20449
αPD1
RK20449 + αPD1

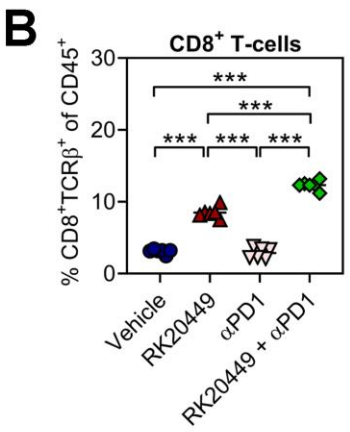
B
CD8+ T-cells
% CD8+TCRβ+ of CD45+
Vehicle
RK20449
αPD1
RK20449 + αPD1

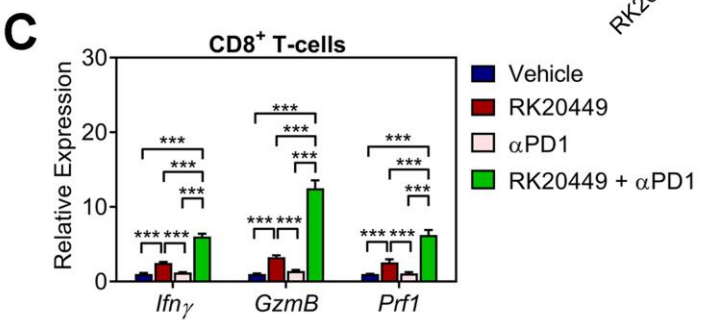
C
CD8+ T-cells
Relative Expression
Ifnγ
GzmB
Prf1
Vehicle
RK20449
αPD1
RK20449 + αPD1

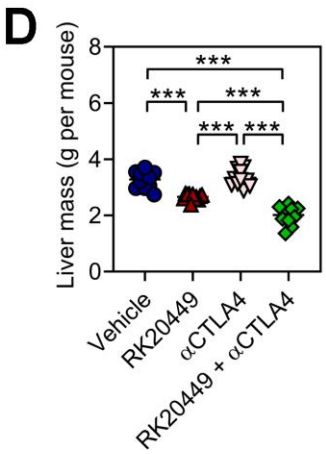
D
Liver mass (g per mouse)
Vehicle
RK20449
αCTLA4
RK20449 + αCTLA4

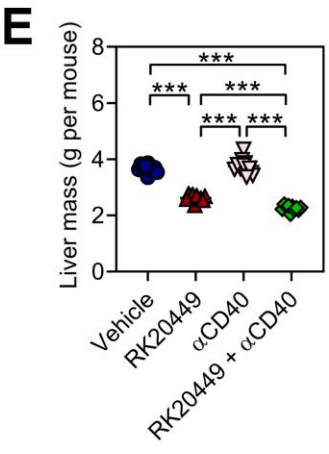
E
Liver mass (g per mouse)
Vehicle
RK20449
αCD40
RK20449 + αCD40

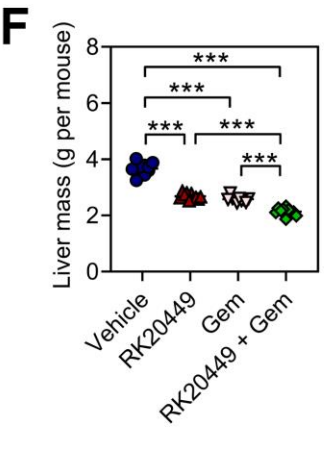
F
Liver mass (g per mouse)
Vehicle
RK20449
Gem
RK20449 + Gem

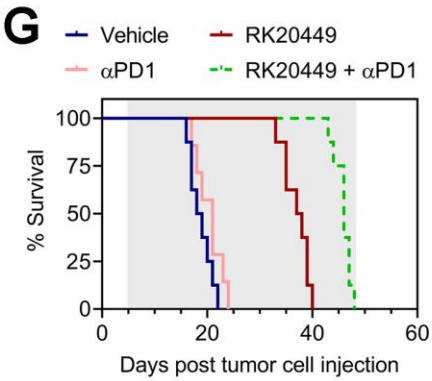
G
Vehicle
RK20449
αPD1
RK20449 + αPD1
% Survival
Days post tumor cell injection

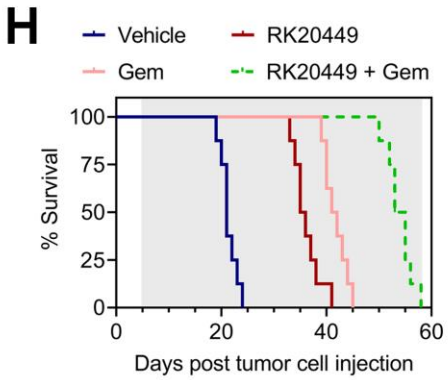
H
Vehicle
RK20449
Gem
RK20449 + Gem
% Survival
Days post tumor cell injection

**Figure S4. Therapeutic inhibition of HCK improves the efficacy of immunotherapy and chemotherapy in PDAC. Related to Figure 4.**

**(A)** Representative whole mounts and corresponding liver weights of WT hosts treated with the small molecule HCK inhibitor RK20449 (twice daily) and/or αPD1 (once every 3 days). Treatment commenced on the 5$^{th}$ day after intrasplenic KPC tumor cell injection and continued for 2 weeks. Scale bar: 1cm. Each symbol represents an individual mouse. n ≥ 11 mice per group.

**(B)** Flow cytometry quantification of CD8$^{+}$ T-cells in KPC liver metastases of WT mice treated as described in Figure S4A. Each symbol represents an individual mouse. n = 6 mice per group.

**(C)** qPCR analysis on CD45$^{+}$TCRβ$^{+}$CD8$^{+}$ T-cells isolated from KPC liver metastases of WT mice treated as described in Figure S4A. n = 4 mice per group.

**(D, E)** Liver weights of WT hosts treated with the small molecule HCK inhibitor RK20449 (twice daily) and/or **(D)** αCTLA4 or **(E)** αCD40 (once every 3 days). Treatment commenced on the 5$^{th}$ day after intrasplenic KPC tumor cell injection and continued for 2 weeks. Each symbol represents an individual mouse. n ≥ 10 mice per group.

**(F)** Liver weights of WT hosts treated with the small molecule HCK inhibitor RK20449 (twice daily) and/or Gemcitabine (weekly). Treatment commenced on the 5$^{th}$ day after intrasplenic KPC tumor cell injection and continued for 2 weeks. Each symbol represents an individual mouse. n = 10 mice per group.

**(G)** Kaplan-Meier survival analysis of WT hosts treated with the small molecule HCK inhibitor RK20449 (twice daily) and/or αPD1 (once every 3 days). Treatment commenced on the 5$^{th}$ day after intrasplenic KPC tumor cell injection and continued until clinical endpoint. Shaded area indicates treatment period. n = 8 mice per group. A Mantel-Cox log-rank test was used to evaluate statistical significance (see Table S10).

**(H)** Kaplan-Meier survival analysis of WT hosts treated with the small molecule HCK inhibitor RK20449 (twice daily) and/or Gemcitabine (weekly). Treatment commenced on the 5$^{th}$ day after intrasplenic KPC tumor cell injection and continued until clinical endpoint. Shaded area indicates treatment period. n = 8 mice per group. A Mantel-Cox log-rank test was used to evaluate statistical significance (see Table S11).

Data represents mean ± SEM; ***$p < 0.001$, with statistical significance determined by one-way ANOVA followed by Tukey's multiple comparison test or Mantel-Cox log-rank test for Kaplan-Meier analysis.

**Table S1. Mantel-Cox log-rank test, related to Figure S1D.**

| | **WT$^{\leftarrow WT}$** | **KO$^{\leftarrow WT}$** | **KO$^{\leftarrow KO}$** | **WT$^{\leftarrow KO}$** |
|---|---|---|---|---|
| **WT$^{\leftarrow WT}$** | - | n.s | *** | *** |
| **KO$^{\leftarrow WT}$** | n.s | - | *** | *** |
| **KO$^{\leftarrow KO}$** | *** | *** | - | n.s |
| **WT$^{\leftarrow KO}$** | *** | *** | n.s | - |

n.s = not significant; ***p < 0.001

**Table S2. Mantel-Cox log-rank test, related to Figure S2B.**

| | ***Hck*$^{KO}$ + IgG** | ***Hck*$^{KO}$ + αCXCR3** | ***Hck*$^{KO}$ + αIL12** |
|---|---|---|---|
| ***Hck*$^{KO}$ + IgG** | - | *** | *** |
| ***Hck*$^{KO}$ + αCXCR3** | *** | - | n.s |
| ***Hck*$^{KO}$ + αIL12** | *** | n.s | - |

n.s = not significant; ***p < 0.001

**Table S3. Mantel-Cox log-rank test, related to Figure 2C.**

| | **WT + RK20449** | **WT + αCSF1R + RK20449** | **cDC1$^{KO}$ + RK20449** | **cDC1$^{KO}$ + αCSF1R + RK20449** |
|---|---|---|---|---|
| **WT + RK20449** | - | n.s | *** | *** |
| **WT + αCSF1R + RK20449** | n.s | - | *** | *** |
| **cDC1$^{KO}$ + RK20449** | *** | *** | - | *** |
| **cDC1$^{KO}$ + αCSF1R + RK20449** | *** | *** | *** | - |

n.s = not significant; ***p < 0.001

**Table S4. Mantel-Cox log-rank test, related to Figure S2C.**

| | **WT** | ***Rag1*$^{KO}$** | ***Hck*$^{KO}$** | ***Hck*$^{KO}$;*Rag1*$^{KO}$** |
|---|---|---|---|---|
| **WT** | - | n.s | *** | *** |
| ***Rag1*$^{KO}$** | n.s | - | *** | *** |
| ***Hck*$^{KO}$** | *** | *** | - | *** |
| ***Hck*$^{KO}$;*Rag1*$^{KO}$** | *** | *** | *** | - |

n.s = not significant; ***p < 0.001

**Table S5. Mantel-Cox log-rank test, related to Figure 2D.**

| | ***Hck*$^{KO}$ + IgG** | ***Hck*$^{KO}$ + αCD4** | ***Hck*$^{KO}$ + αCD8** | ***Hck*$^{KO}$ + αNK1.1** |
|---|---|---|---|---|
| ***Hck*$^{KO}$ + IgG** | - | *** | *** | *** |
| ***Hck*$^{KO}$ + αCD4** | *** | - | *** | ** |
| ***Hck*$^{KO}$ + αCD8** | *** | *** | - | *** |
| ***Hck*$^{KO}$ + αNK1.1** | *** | ** | *** | - |

**p < 0.01, ***p < 0.001

**Table S6. Mantel-Cox log-rank test, related to Figure 4B.**

| | WT + IgG | *Hck*$^{KO}$ + IgG | WT + αPD1 | *Hck*$^{KO}$ + αPD1 |
|---|---|---|---|---|
| **WT + IgG** | - | *** | n.s | *** |
| ***Hck*$^{KO}$ + IgG** | *** | - | *** | *** |
| **WT + αPD1** | n.s | *** | - | *** |
| ***Hck*$^{KO}$ + αPD1** | *** | *** | *** | - |

n.s = not significant; ***p < 0.001

**Table S7. Mantel-Cox log-rank test, related to Figure 4D.**

| | WT + IgG | *Hck*$^{KO}$ + IgG | WT + αCTLA4 | *Hck*$^{KO}$ + αCTLA4 |
|---|---|---|---|---|
| **WT + IgG** | - | *** | n.s | *** |
| ***Hck*$^{KO}$ + IgG** | *** | - | *** | *** |
| **WT + αCTLA4** | n.s | *** | - | *** |
| ***Hck*$^{KO}$ + αCTLA4** | *** | *** | *** | - |

n.s = not significant; ***p < 0.001

**Table S8. Mantel-Cox log-rank test, related to Figure 4F.**

| | WT + IgG | *Hck*$^{KO}$ + IgG | WT + αCD40 | *Hck*$^{KO}$ + αCD40 |
|---|---|---|---|---|
| **WT + IgG** | - | *** | n.s | *** |
| ***Hck*$^{KO}$ + IgG** | *** | - | *** | *** |
| **WT + αCD40** | n.s | *** | - | *** |
| ***Hck*$^{KO}$ + αCD40** | *** | *** | *** | - |

n.s = not significant; ***p < 0.001

**Table S9. Mantel-Cox log-rank test, related to Figure 4H.**

| | WT + Vehicle | *Hck*$^{KO}$ + Vehicle | WT + Gem | *Hck*$^{KO}$ + Gem |
|---|---|---|---|---|
| **WT + Vehicle** | - | *** | *** | *** |
| ***Hck*$^{KO}$ + Vehicle** | *** | - | n.s | *** |
| **WT + Gem** | *** | n.s | - | *** |
| ***Hck*$^{KO}$ + Gem** | *** | *** | *** | - |

n.s = not significant; ***p < 0.001

**Table S10. Mantel-Cox log-rank test, related to Figure S4G.**

| | Vehicle | RK20449 | αPD1 | RK20449 + αPD1 |
|---|---|---|---|---|
| **Vehicle** | - | *** | n.s | *** |
| **RK20449** | *** | - | *** | *** |
| **αPD1** | n.s | *** | - | *** |
| **RK20449 + αPD1** | *** | *** | *** | - |

n.s = not significant; ***p < 0.001

**Table S11. Mantel-Cox log-rank test, related to Figure S4H.**

| | Vehicle | RK20449 | Gem | RK20449 + Gem |
|---|---|---|---|---|
| **Vehicle** | - | *** | *** | *** |
| **RK20449** | *** | - | ** | *** |
| **Gem** | *** | ** | - | *** |
| **RK20449 + Gem** | *** | *** | *** | - |

**p < 0.01, ***p < 0.001

**Table S12. Taqman probes for qPCR analysis, related to STAR Methods.**

| Probe ID (Gene) | Source | Identifier |
|---|---|---|
| *18s* | ThermoFisher | Mm04277571_s1 |
| *Gapdh* | ThermoFisher | Mm99999915_g1 |
| *Hck* | ThermoFisher | Mm01241463_m1 |
| *Il4* | ThermoFisher | Mm00445259_m1 |
| *Il6* | ThermoFisher | Mm00446190_m1 |
| *Il10* | ThermoFisher | Mm01288386_m1 |
| *Il11* | ThermoFisher | Mm00434162_m1 |
| *Il13* | ThermoFisher | Mm00434204_m1 |
| *Arg1* | ThermoFisher | Mm00475988_m1 |
| *Tgfβ* | ThermoFisher | Mm01227699_m1 |
| *Il12α* | ThermoFisher | Mm00434169_m1 |
| *Ifnγ* | ThermoFisher | Mm01168134_m1 |
| *Cxcl9* | ThermoFisher | Mm00434946_m1 |
| *Cxcl10* | ThermoFisher | Mm00445235_m1 |
| *Tnf* | ThermoFisher | Mm00443258_m1 |
| *Prf1* | ThermoFisher | Mm00812512_m1 |
| *GzmB* | ThermoFisher | Mm00442837_m1 |
| *Mmp3* | ThermoFisher | Mm00440295_m1 |
| *Mmp7* | ThermoFisher | Mm00487724_m1 |
| *Mmp9* | ThermoFisher | Mm00442991_m1 |
| *Col1a1* | ThermoFisher | Mm00801666_g1 |